EARTHQUAKE ENGINEERING AND STRUCTURAL DYNAMICS
Earthquake Engng. Struct. Dyn. **28**, 785–803 (1999)

SEISMIC STABILITY AND THE FORCE REDUCTION FACTOR OF CODE-DESIGNED ONE-STOREY ASYMMETRIC STRUCTURES

MARIO DE STEFANO[1,*] AND AVIGDOR RUTENBERG[2]

[1]*Dipartimento di Costruzioni, Università di Firenze, Piazza Brunelleschi 6, 50121 Firenze, Italy*
[2]*Department of Civil Engineering, Technion - Israel Institute of Technology, Haifa 32000, Israel*

SUMMARY

This paper evaluates the stability bounds of the force reduction factor R of unidirectionally loaded UBC designed asymmetric one-storey systems having different mass and stiffness distributions. It is shown that whereas the instability effects due to torsional response are neutralized by the asymmetry-related over-strength, instability bounds may still be lower than the R-values prescribed by the code. Results of a limited study indicate that bidirectional ground motion tends to reduce further the safety margin against dynamic instability. Copyright © 1999 John Wiley & Sons, Ltd.

KEY WORDS: dynamic instability; code design; yielding asymmetric structures; unidirectional and bidirectional excitation

INTRODUCTION

As is known, most structures are designed to yield under strong earthquake action, but to avoid collapse it is necessary to provide — mainly through proper detailing — adequate ductility supply. The force reduction (or the response modification) factor R specified in seismic codes is a measure of this supply.

The action of gravity loads on the laterally displaced configuration of the structure (gravity, P–Δ or instability effects) can lead to earlier collapse due to inordinate increase in the lateral deflections and, hence, in the ductility demand when the post-yield stiffness, as modified by gravity effects, is negative. Therefore, when substantial gravity effects are present, the strength of the structure may not be sufficient to limit the deflections to an acceptable level. It follows that the onset of seismic instability imposes an upper bound on R, which may be lower than the values prescribed in seismic codes. Moreover, in torsionally unbalanced systems, destabilizing torques

* Correspondence to: Mario De Stefano, Dipartimento di Costruzioni, Università di Firenze, Piazza Brunelleschi 6, 50121 Firenze, Italy

Contract/grant sponsor: Italian CNR
Contract/grant sponsor: Israeli Ministry of Contruction and Housing

CCC 0098–8847/99/070785–19$17·50

Received 2 December 1997
Revised 18 August 1998 and 7 January 1999

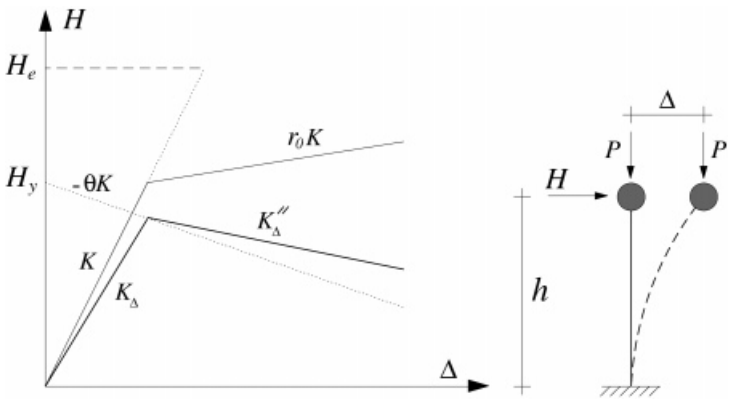

Figure 1. Force–displacement relation accounting for P–Δ effects

due to floor rotations lower this bound even further. However, because of its threshold nature, this upper bound or limiting value of R, R_1, can not be substituted for the code value, but it can be taken as a basis for a further reduced design value.

The effect of gravity on the lateral force–displacement relation of a Single-Degree-of-Freedom (SDOF) system with a positive secondary slope ($= r_0K$, where $K =$ elastic stiffness) is shown in Figure 1. Such a system can become unstable only when the secondary slope, as modified by the P–Δ effects, becomes negative. The classical elastic buckling load $\approx Kh$ is usually very much larger than the dynamic instability threshold, and is not considered here.

From Figure 1, it can be seen that the secondary slope, as modified by gravity, K_Δ is given by

$$K_\Delta = K_0(r_0 - \theta) = -K\theta_{\text{eff}} = K_\Delta \frac{r_0 - \theta}{1 - \theta} \tag{1}$$

where $\theta = P/(Kh)$ is the stability coefficient, $\theta_{\text{eff}} = \theta - r_0$ is the so-called effective stability coefficient and $K_\Delta = K\,(1 - \theta)$ is the second-order primary stiffness.

In the equivalent lateral force and modal analysis procedures advocated by seismic codes, P–Δ effects have traditionally been taken into account through an amplification factor given by $1/(1 - \theta)$, or in some codes by $1/(1 - R_d\theta)$, R_d being the deflection amplification factor, which in the U.S. practice is somewhat smaller than R. A discussion of the relative merits of these two formulas is given in the Commentary to the NEHRP Recommended Provisions.[1]

However, it was apparent that such a simplistic approach can not produce reliable predictions of the seismic response of gravity affected yielding structures, and therefore dynamic procedures became necessary. Most of the proposed procedures aim at evaluating the strength level — considering gravity effects — that is required to result in the same ductility demand as that obtained without gravity. Bernal[2] and Cosenza *et al.*[3] are perhaps the earliest proponents of this approach. Bernal[2] also noted that a bound on peak ductility demand should be set in order to ensure that residual post-earthquake deformations would not impair the gravity load capacity of the system. In a later paper, Bernal[4] also presented statistically derived expressions to predict the strength at the threshold of instability, which will be referred to subsequently. Similar studies were carried out by other investigators (e.g. References 5 and 6).

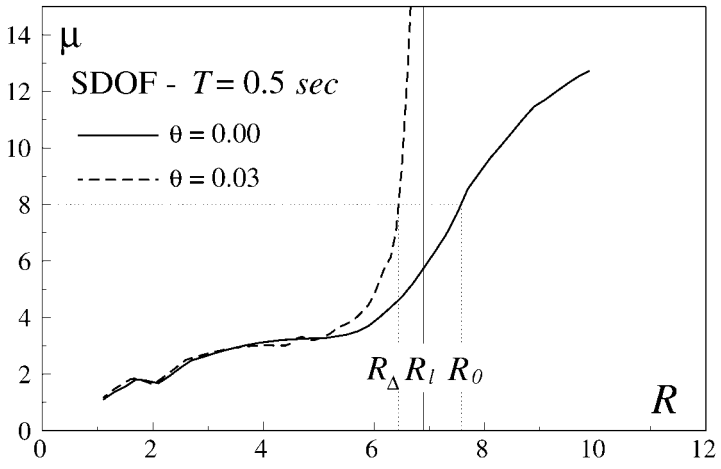

Figure 2. Definition of R_0, R_I and R_Δ

Whereas the majority of these studies focused on elastic–perfectly plastic or bilinear hardening behaviour, gravity effects on degrading systems were also studied.[4–7] It was concluded that the destabilizing gravity effects are lesser for stiffness degrading systems than for bilinear ones. Priestley *et al.*[8] also observed that the unloading stiffness is one of the main parameters governing the stability of these structures. It is thus seen that, when more realistic response relationship is assumed, gravity effects become less pronounced than for elastic–perfectly plastic systems.

Extensions of some of the procedures to multistorey structures were made by several investigators.[4,9,10] A survey of several static and dynamic methods was made by MacRae.[6]

It is well known that gravity effects are not significant unless R is close to R_I (its limiting value); therefore, accounting for these effects by calibrating the required increase in system strength to obtain the same ductility demand as without these effects does not necessarily guarantee adequate safety against dynamic instability. This can clearly be seen from Figure 2, where a typical ductility demand μ vs. the reduction factor R curve is shown for an SDOF system subjected to the 1940 El Centro record (S00E component). Let R_0 and R_Δ denote, respectively, the force reduction factors, without and with gravity effects, at a given ductility demand level μ; then, when $R_0 < R_I$, one can expect a larger safety factor SF against instability ($SF = R_I/R_\Delta$) than when $R_0 > R_I$. This is further demonstrated in Figure 3, where the mean and mean minus one standard deviation (mean-σ) SF spectra for $\mu = 4$, 6 and 8 are presented for the first El Centro record and the other four records listed in Table I. It appears that SF values are scattered with respect to their means. This is due to the fact that SF is generally found to be high for Petrovac and Tolmezzo that are of shorter duration, and relatively low for El Centro, Taft and Valparaiso. On the whole, it can be seen that the (mean-σ) SF values are very low for the higher ductility systems, which are commonly considered by structural engineers.

More recent papers studied the response at the onset of instability of torsionally unbalanced systems, for which floor rotations induce destabilizing torques, thereby further amplifying the gravity effects. Sordo and Bernal,[11] using an equivalent SDOF model, concluded that seismic torsional instability is not likely to be significantly affected by torsional eccentricity provided that

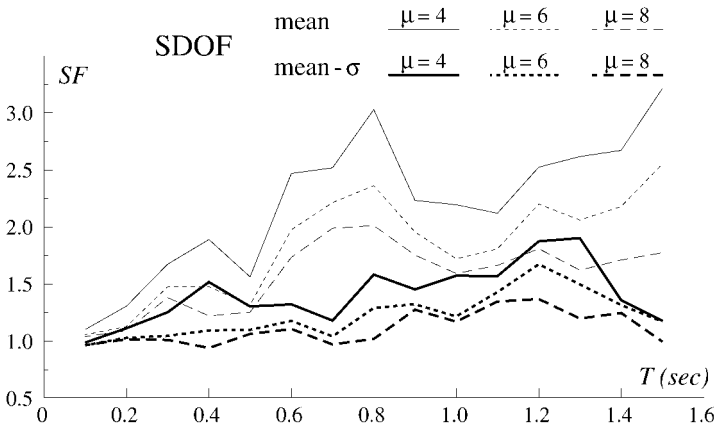

Figure 3. Mean and (mean-σ) *SF* spectra

Table I. Characteristics of the selected earthquake records

Earthquake	Record	Component	Duration (sec)	PGA (g)	PGV (m/sec)
Imp. Valley 1940	El Centro	S00E	53·8	0·348	0·334
Imp. Valley 1940	El Centro	S90W	53·8	0·214	0·369
Montenegro 1979	Petrovac	NS	19·6	0·438	0·413
Taft 1952	Lincoln Tunnel	S69E	54·4	0·179	0·177
Friuli 1976	Tolmezzo	EW	36·4	0·313	0·300
Chile 1985	Valparaiso	N50E	72·0	0·284	0·264

PGA = Peak Ground Acceleration; PGV = Peak Ground Velocity

the overstrengths of the various elements do not significantly deviate from the system average, but when this condition is not satisfied, failure occurs by pivoting about the strong element. Subsequently, Sordo and Bernal[12] studied the general characteristics of the response at the instability threshold of one-storey asymmetric systems under bidirectional ground motion. A methodology for predicting collapse intensities of the earthquake record was developed and tested numerically.

The aim of this study is mainly to present results of studies on the effect of asymmetry on the instability bounds in one-storey structures that are code-designed in the sense that the *distribution* of strength among the resisting elements follows the seismic provisions of the UBC.[13] However, they are not strictly code-designed, since their strength is based on the spectral ordinate of the particular ground motion record considered, rather than on that of the design spectrum. With a number of time histories this approach is similar to record scaling to match code spectral ordinates. The effects of asymmetry on the limiting reduction factor R_1 is evaluated by parametric studies on the *unidirectional* response of models designed by the seismic provisions of the UBC[13] and excited by unidirectional ground motion, i.e. the models used extensively in torsional

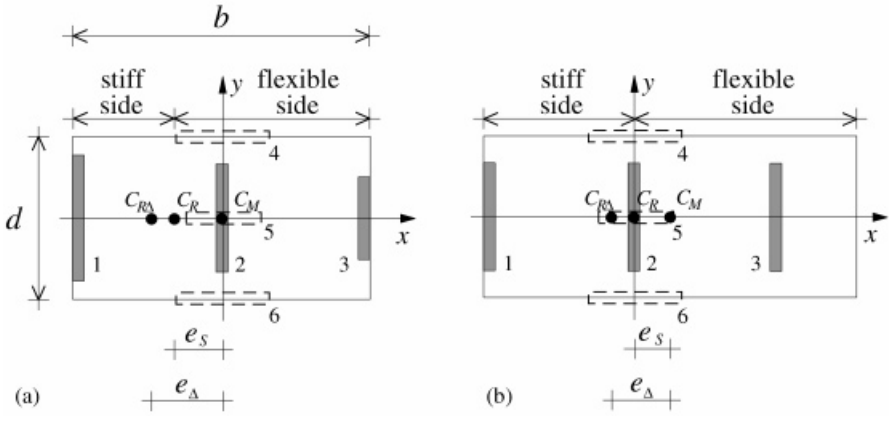

Figure 4. Idealized one-storey systems: (a) stiffness eccentric CM model and (b) mass eccentric SME model

response studies (e.g. References 14 and 15). By analysing such 'standard' models it becomes easier to assess the significance of instability, as measured by the effective stability coefficient θ_{eff} (> 0) (Figure 1), with variations in the main system parameters, namely the uncoupled lateral period of the system T, stiffness eccentricity e_S and torsional-to-lateral frequency ratio Ω. A limited investigation has been conducted to compare the effects of model characteristics, i.e. stiffness eccentric vs. mass eccentric models, on the response. Also, a number of analyses have been carried out to assess the effects of *bidirectional* excitation on failure modes and stability thresholds. Several earthquake time histories, all typical of stiff soil conditions, are considered in order to obtain a range of expected values and gain some confidence in the results.

IDEALIZED MODELS

The models investigated in the present study are monosymmetric one-storey structures, the floor plan and resisting elements of which are shown in Figure 4. For unidirectional excitation in the asymmetric y-direction — with which this paper is mainly concerned — only elements parallel to y are assumed to resist lateral loading. A preliminary study of bidirectional effects was also made, and for this case x-direction elements, as shown in Figure 4 in broken lines, were added. These elements carry loads acting along x, and also resist part of the torques from the y-direction loading. Modelling monosymmetric structures excited unidirectionally without x-direction elements located at or near the periphery is not very realistic. Yet, it is consistent with findings of Correnza *et al.*[16] and De la Llera and Chopra[17] that, when the x-component of the ground motion produces long intervals of yielding in elements aligned in this direction, their contribution to resisting the y-direction induced torques is not significant and may be disregarded. It is also assumed that the mass is uniformly distributed with the centroid at C_M and the floor slab is rigid in its own plane. The distance from the stiffness centre C_R to C_M, both located on the x-axis, is the stiffness eccentricity e_S. Furthermore, the response of all resisting elements, which provide stiffness and strength in their own plane only, is taken as elastic–perfectly plastic.

In Figure 4(a) the elements are arranged so that C_M lies in the line of action of Element 2. This stiffness eccentric system is sometimes denoted as the CM model. In Figure 4(b) the elements are symmetrically located with respect to C_R, and the eccentricity is effected by shifting C_M from C_R. This is the mass eccentric or SME model. In fact, for rectangular floor plans — implying practically uniform mass distribution along the x-axis — mass eccentric systems with a large eccentricity are less realistic than stiffness eccentric ones since, for the former ones, a symmetric stiffness arrangement, with respect to an axis which is not an axis of symmetry, results in the absence of resisting elements near one edge of the floor slab, as is evident from Figure 4(b).

In order to understand the effect of gravity loads on the response of these asymmetric structures, it may be useful to describe their behaviour in the linear range before embarking on the study of their dynamic non-linear response.

The equilibrium equations, including the P–Δ effects, with respect to C_M, which herein is also the centre of gravity, for a shear force F_0 acting at C_M, are given by

$$\left(\begin{bmatrix} K & Ke_S \\ Ke_S & K_\phi + Ke_S^2 \end{bmatrix} - \frac{P}{h} \begin{bmatrix} 1 & 0 \\ 0 & \rho^2 \end{bmatrix} \right) \begin{Bmatrix} y \\ \phi \end{Bmatrix} = \begin{Bmatrix} F_0 \\ 0 \end{Bmatrix} \tag{2}$$

where K = lateral stiffness of system, K_ϕ = torsional rigidity with respect to C_R, y = lateral displacement, ρ = gravity load distribution radius w.r.t. to C_M, which is also assumed to be the mass radius of gyration, and ϕ = angle of twist assumed positive when counter-clockwise. Since the centre of gravity is located at C_M, the second-order centre of rigidity $C_{R\Delta}$, i.e. the centre of rigidity considering $P-\Delta$ effects, does not coincide with C_R. Its location can easily be computed by considering the effect of gravity as a fictitious element with negative stiffness located at C_M.[18] It can then be shown that the centre $C_{R\Delta}$ of the second-order stiffness $K_\Delta = K - P/h$ is located at a distance $e_\Delta = e_S/(1-\theta)$ from C_M (Figure 4), i.e. the distance of $C_{R\Delta}$ from C_R $\Delta e = e_S\theta/(1-\theta)$. Shifting the origin of the co-ordinate system to $C_{R\Delta}$ uncouples the two equations (2), and leads to the following expression for the second-order torsional rigidity w.r.t. $C_{R\Delta}$:

$$K_{\phi\Delta} = K_\phi - K\theta\left(\frac{e_S^2}{1-\theta} + \rho^2\right) \tag{3}$$

It is thus seen that, in addition to the reduction in the translational rigidity, the effects of gravity on asymmetric systems are manifested through a lowered torsional rigidity and through a shift in the location of centre of rigidity. Note that this shift is associated with an additional torque $\Delta M = F_0\Delta e$.

For yielding structures the problem is somewhat more involved since element strengths should also be considered. These strengths F_i are routinely allocated on the basis of the well-known static formula

$$F_i = F_0\left[\frac{k_i}{K} + \frac{e_d a_i k_i}{K_\phi}\right], \quad i = 1, 2, 3 \tag{4}$$

in which F_0 = design base shear (herein the spectral acceleration ordinate divided by R), k_i = lateral (herein y-direction) stiffness of the ith element, a_i = its perpendicular distance from C_R, e_d = design or load eccentricity from C_R. In code-designed structures, $e_d \neq e_S$, as will be seen subsequently. Note that the difference in the strength-to-stiffness ratios of the elements leads to multi-linear force–displacement and torque–rotation relationships. Also, with element plastification, C_R and $C_{R\Delta}$ move from their original locations, leading to varying eccentricities for the

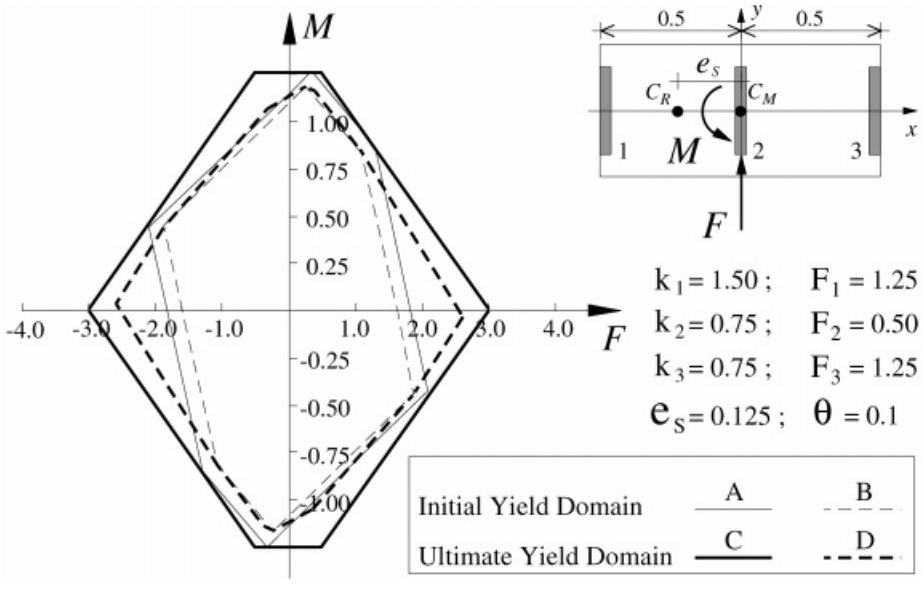

Figure 5. Shear–torque yield surfaces with and without P–Δ effects

incremental shear forces.[18] Whereas these two response relationships define the system as it plastifies, perhaps more insight into the static behaviour of monosymmetric systems can be gained from the shear F — torque M yield surfaces or interaction curves. Typical surfaces with respect to C_M for a stiffness eccentric — strength symmetric (i.e. the plastic centroid is located at C_M) model used by De la Llera and Chopra[17] are shown in Figure 5. The polygon A is the limiting elastic first-order shear–torque locus and polygon B is its second-order counterpart. Polygons C and D are the first- and second-order ultimate yield surfaces, respectively. At ultimate yield, the shear–torque combinations plot along C or D, whereas during partial yielding the shear–torque combinations plot in the area between curves A and C or B and D depending on whether or not gravity effects are considered. As expected, gravity effects lower the elastic as well as the plastic capacities of the system.

STRENGTH DESIGN

In order to provide structures with more favourable strength distributions, as well as over-strength, all seismic codes require — for design purposes — shifting C_M to a new location with an eccentricity e_d ($\neq e_S$). In the UBC,[13] which is the code chosen for the present parametric study, e_d is given by:

$$e_d = e + 0{\cdot}05A_x b \tag{5}$$

$$e_d = e - 0{\cdot}05A_x b \leqslant 0 \tag{6}$$

in which b is the building dimension perpendicular to the direction of excitation, and A_x, the eccentricity amplification factor, is given by:

$$1{\cdot}0 \leqslant A_x = \left(\frac{\delta_{\max}}{1{\cdot}2\delta_{\text{avg}}}\right)^2 \leqslant 3{\cdot}0 \tag{7}$$

where $\delta_{\max}$ = maximum lateral displacement of the floor at the considered level, $\delta_{\text{avg}} = (\delta_{\max} + \delta_{\min})/2$, and $\delta_{\min}$ = minimum lateral floor displacement. In other words, when $\delta_{\max} \leqslant 1{\cdot}5\ \delta_{\min}$, $A_x = 1{\cdot}0$ and, when $\delta_{\max} \cdot \delta_{\min} \leqslant 0$, $A_x = 3{\cdot}0$. A more severe load combination for each element resulting from using either equation (5) or (6) shall be considered in design. Note that $\delta_{\max}$ and $\delta_{\min}$ are to be computed based on e_{d} obtained from equation (5) for $A_x = 1{\cdot}0$. The rationale for incorporating an amplification factor A_x in the design eccentricity expressions is given by the NEHRP Commentary,[1] as based on indications that the $0{\cdot}05\ b$ (i.e. $A_x = 1{\cdot}0$) accidental eccentricity may not be adequate for protecting the structure against torsional instability.

From the $\leqslant 0$ condition in equation (6), it follows that strengths should not be decreased due to torsional effects. Apparently, this has been the common interpretation of the UBC provisions. However, in the Commentary to the 1996 edition of the Structural Engineers Association of California code,[19] it is explicitly stated that such a decrease is permissible, i.e. the $\leqslant 0$ condition is removed. This results in a somewhat less conservative design for elements located on the rigid side of the floor deck.[20,21] In the present study, however, the 'common' interpretation is applied.

Once e_{d} has been obtained, the code-specified element strengths are evaluated by substitution into equation (4). However, for parametric studies it is useful to normalize the length dimensions with respect to the mass radius of gyration about C_{M}, ρ, so that the results are not dependent on the absolute dimensions of the floor slab. Letting $a_i^* = a_i/\rho$, $e_{\text{d}}^* = e_{\text{d}}/\rho$ and $\Omega^2 = K_\phi/(K\rho^2)$, equation (4) takes the following form:

$$F_i = F_0 \frac{k_i}{K}\left[1 + \frac{e_{\text{d}}{*}a_i{*}}{\Omega^2}\right] \tag{8}$$

It is well known that, since e_{d} takes different values for elements located on either side of the floor, $\sum F_i > F_0$, i.e. an overstrength $OS = \sum F_i/F_0$ exists relative to the pure symmetric or torsionally balanced case. This overstrength may be quite large for torsionally flexible systems, i.e. systems having Ω, which is the uncoupled torsional-to-lateral frequency ratio, smaller than unity. For example, when the CM model shown in Figure 4 has $\Omega = 0{\cdot}6$ and $e^* = e/\rho = 0{\cdot}25$, then $OS = 1{\cdot}55$. In other words, the force reduction factor R, i.e. the ratio of the required elastic strength to the design strength, is lowered to 65% of its original value. Since the strength increase affects more the edge elements, which are usually the critical ones, the expected reduction in the ductility demand (as based on the equal displacement assumption) is similar. On the other hand, for $\Omega = 1{\cdot}4$ and $e^* = 0{\cdot}25$, $OS = 1{\cdot}14$. Furthermore, the code overstrength increases with the normalized eccentricity e^* of the system, whereas it remains constant as the system uncoupled lateral period $T = 2\pi\sqrt{M/K}$ changes.

Note that since no uncertainties in defining element properties and mass distribution and no rotational ground motion were specified, accidental eccentricity should not have been included in e_{d} when strength per equation (8) was allocated, i.e. including the term $0{\cdot}05b$ in e_{d} is not conservative. Whereas this argument is evidently valid, and should be taken into consideration, such an approach would result in studying a model which is different from the one being

Table II. Ω, e^* and OS for systems studied unidirectionally

Model	Ω	e^*	OS	Ω	e^*	OS	Ω	e^*	OS
	0·8	0·25	1·319	1·0	0·25	1·199	1·25	0·25	1·157
CM	0·8	0·50	1·524	1·0	0·50	1·361	1·25	0·50	1·270
	0·8	0·75	1·713	1·0	0·75	1·488	1·25	0·75	1·353
SME	0·8	0·50	1·349	1·0	0·50	1·302	1·25	0·50	1·258

investigated. This, however, is a controversial issue which has been discussed at some length in the literature (e.g. Reference 22).

SYSTEM PARAMETERS

For systems under unidirectional excitation, the stability effects were examined mainly for a range of CM models (Figure 4(a)). This was effected by varying the parameters Ω and e^* within their expected ranges: $\Omega = 0{\cdot}8,\ 1{\cdot}0,\ 1{\cdot}25$; $e^* = 0{\cdot}25,\ 0{\cdot}50,\ 0{\cdot}75$. Note that for rectangular buildings loaded normal to their larger plan dimension the width b ranges between $2{\cdot}5\rho$ and $3{\cdot}5\rho$, i.e. $e^* = 0{\cdot}75$ corresponds to $0{\cdot}2b \leqslant e \leqslant 0{\cdot}3b$, and is a large eccentricity. Herein $b = 3\rho$.

Table II lists nine CM models thus created, and for comparison also three SME ones (Figure 4(b)) with $e^* = 0{\cdot}50$. It can be seen that the system overstrength OS increases with falling Ω and increasing e^*. As will be demonstrated subsequently, this property is responsible for the very weak dependence of R_1 on Ω and e^*. In all these cases R_1 was evaluated for a range of the fundamental period $T: 0{\cdot}1 \leqslant T \leqslant 1{\cdot}5$ sec. Systems with code overstrength as well as strength-normalized ones (i.e. with no OS) were analysed: the former were used to examine the response of actual systems, the latter ones were studied to better understand the influence of system parameters Ω and e^* on stability. For comparison, reference symmetric models, i.e. the SDOF systems having a fundamental period equal to the uncoupled period of the considered asymmetric systems, were also analysed.

For systems under bidirectional excitation a CM model with three elements in each of the two directions was chosen. The layout in the x-direction is symmetric (Figure 4) with the edge Elements 4 and 6 contributing 30 per cent to the total torsional rigidity of the system. The lateral stiffnesses in the two directions are equal so that $T_x = T_y = T$. Typical parameters were chosen for this limited study: $\Omega = 1{\cdot}0$ and $e^* = 0{\cdot}5$. Routine calculations using equation (4) or (8) in each of the two directions led to $OS_y = 1{\cdot}31$ and $OS_x = 1{\cdot}09$, the latter value being based on an accidental eccentricity of 0.05 d (d = floor plan dimension along y, Figure 4), as $A_x = 1.0$ per equation (7).

The design base shear strengths (F_o) along y and x have been taken first as the spectral acceleration values of the relevant earthquake component at the system uncoupled period T, i.e. the strength along y is obtained from the spectral ordinate of the earthquake component which is selected as the y-input ground motion, and similarly for the x-direction. However, this approach leads to different strengths in the two directions, a result that for $T_x = T_y$ may not be compatible with actual designs in which the spectral ordinates in each direction match the respective natural periods on the same design spectrum. Therefore, a parallel parametric study based on equal base

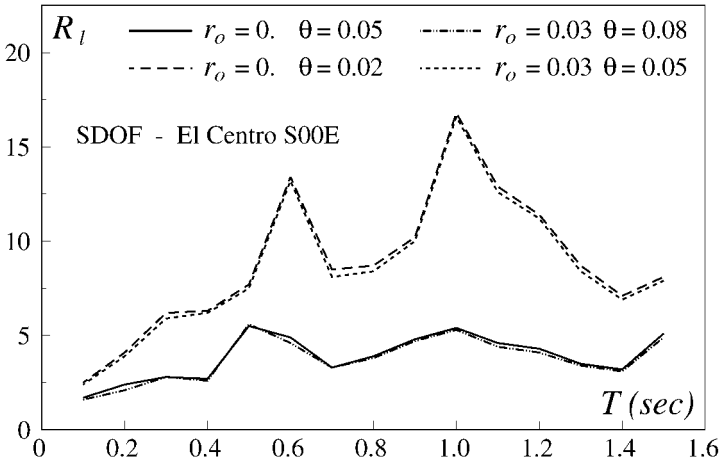

Figure 6. Effect of θ_{eff} on the limiting reduction factor R_1

shear strengths was also made. With the latter approach *OS* is also a function of the period T, but the effect is mostly on Elements 4 and 6, since the x-direction ground motion component has been taken as the one with the smaller Peak Ground Acceleration (PGA).

It is known[6,23] that the onset of instability is governed by the parameter $\theta_{\text{eff}} = \theta - r_0$ (Figure 1). This is confirmed in Figure 6 where the variation in R_1 with the period is shown for EPP (elastic–perfectly plastic) SDOF systems, assuming $\theta_{\text{eff}} = \theta = 0{\cdot}02$ and $0{\cdot}05$, and for bilinear hardening SDOF systems with $r_0 = 0{\cdot}03$ and $\theta = 0{\cdot}05$ and $0{\cdot}08$, such that they are characterized by the same θ_{eff} as the EPP models. The curves present values of R_1 that are practically coincident for EPP and bilinear systems having the same θ_{eff}, whereas, as expected, R_1 is very sensitive to the variation in θ_{eff}. Therefore, the slight change in the initial period T, due to the different θs selected for EPP and bilinear models, has practically no effect on the onset of dynamic instability.[9] In view of the above observations, the analysis has been carried out only for EPP systems, i.e. for $\theta_{\text{eff}} = \theta$.

The value of θ depends on P (gravity load), which in turn is related to the natural period T. Following Bernal,[2] θ is taken as the ratio of the admissible interstorey drift ratio to the seismic design coefficient. Using the UBC[13] expressions for these two parameters leads to:

$$\theta = \min(0{\cdot}005;\ 0{\cdot}04/R_{\text{w}})\,\frac{T^{2/3}R_{\text{w}}}{1{\cdot}25ZIS}, \quad T \leqslant 0{\cdot}7 \text{ sec} \tag{9a}$$

$$\theta = \min(0{\cdot}004;\ 0{\cdot}003/R_{\text{w}})\,\frac{T^{2/3}R_{\text{w}}}{1{\cdot}25ZIS}, \quad T > 0{\cdot}7 \text{ sec} \tag{9b}$$

in which R_{w} = force reduction factor at working load level, Z = seismic zone factor, I = importance factor and S = site coefficient. For $I = S = 1{\cdot}0$ and a given T, θ depends on Z and on R_{w} when its value is smaller than $8{\cdot}0$ (equation (9a)) or $7{\cdot}5$ (equation (9b)). To reduce the number of parameters in the study, the analysis was confined to the largest value of R_{w} considered by the UBC, i.e. $R_{\text{w}} = 12$. Evidently, the lower the value of Z the higher is θ. Yet, the maximum value of Z ($Z = 0{\cdot}4$) was chosen in order to demonstrate that, even for very low θ, the resulting R_1 for

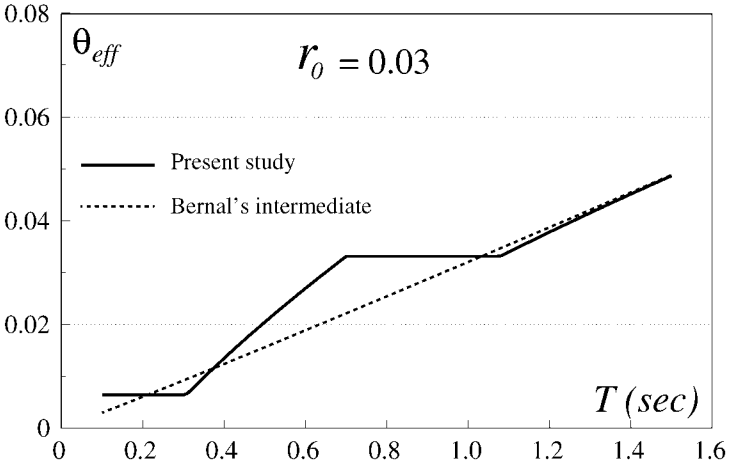

Figure 7. Assumed variation in θ_{eff} with fundamental period T

structures with relatively large ductility supply can already be quite low, so that designs with high R_{w} values may not be safe. There was also concern about the effect of T on R_{I}, albeit some contrary evidence.[4] On the other hand, since equations (9) are based on the maximum drift limits, usual drift values are likely to be lower, so that the θ values resulting from the above assumptions represent upper bounds for a given zone. Since for 0·7 sec $< T <$ 1·08 sec, the use of equation (9b) results in θ values lower than those obtained from equation (9a), it was assumed that in this range $\theta = \theta\,(T = 0{\cdot}7$ sec, from equation (9a)). Figure 7 shows θ_{eff} vs. T for $r_0 = 0{\cdot}03$, which is believed to be a realistic ratio for the secondary slope of structures with bilinear force–displacement response (e.g. steel). Note that for bidirectional excitation it was assumed that $\theta_{\text{eff},x} = \theta_{\text{eff},y} = \theta_{\text{eff}}$. In Figure 7 the variation in θ_{eff} with T is compared with an expression proposed by Sordo and Bernal[12] to represent intermediate values of the stability coefficient, namely

$$\theta_{\text{eff}} = 0{\cdot}032T^{1{\cdot}04} \tag{10}$$

It is seen in Figure 7 that the two formulations lead to similar values of θ_{eff}.

For the unidirectional response analysis of the nine CM models, the major horizontal components (i.e. those characterized by the larger peak ground acceleration) of the five earthquakes, as listed in Table I, were chosen as input ground motions, all apparently having similar frequency content characteristics as measured by their similar a/v (a = PGA, v = PGV) ratios, which were close to unity, and are representative of stiff soil conditions. Note that the Petrovac record is relatively short, while the Tolmezzo one is of intermediate length. For the analysis of the three SME models only the S00E component of the El Centro record was used.

Bidirectional analyses were carried out for systems subjected only to the two horizontal components (S00E and S90W, as listed in Table I) of El Centro. The system response under unidirectional excitation was analysed by a version of the computer code DRAIN-2D,[24] and the effect of the geometric stiffness matrix was considered by means of fictitious elements with negative stiffness properties.[18] The bidirectional response was analysed by the computer code

ANSR-I.[25] In all cases, 5 per cent damping was assumed for the two coupled modes of vibration, as well as for the x-direction mode.

For most of the study the response parameter of interest is the limiting force reduction factor R_1, and therefore the results can be directly related to the strength levels required by seismic codes. Time histories of element ductility demands along both x- and y-directions are also presented in order to identify failure modes.

RESULTS FOR UNIDIRECTIONAL EXCITATION

Before presenting the results of the parametric study, it may be interesting to see the effects of torsional stiffness, as represented by Ω, on the system collapse mechanism, and of e^* and Ω on the limiting reduction factor R_1. Figure 8 shows the El Centro ductility demand histories μ of the three elements of two CM models ($\Omega = 1{\cdot}00$ and $1{\cdot}40$, respectively, $T = 0{\cdot}5$ sec) designed for a force reduction factor $R = 9$, i.e. a reduction factor larger than the relevant stability threshold R_1 (Figure 2). The systems were designed without code overstrength in order to isolate the effect of the variation in Ω.

From Figure 8 it can be seen that for $\Omega = 1{\cdot}00$ the ductility demand of Element 3 is becoming quite large after 6 sec, and at failure the floor slab clearly pivots about Element 1 (the strong one). For $\Omega = 1{\cdot}40$, i.e. practically twice the rotational stiffness, the ductility levels are lower and the failure mode is more translational. Note, however, that a pronounced pivoting instability mode does not necessarily imply a large reduction in R_1, since for $\Omega = 1{\cdot}00$ $R_1 = 5{\cdot}5$, whereas for $\Omega = 1{\cdot}40$ $R_1 = 6{\cdot}1$ (these values of R_1 do not include code overstrength OS).

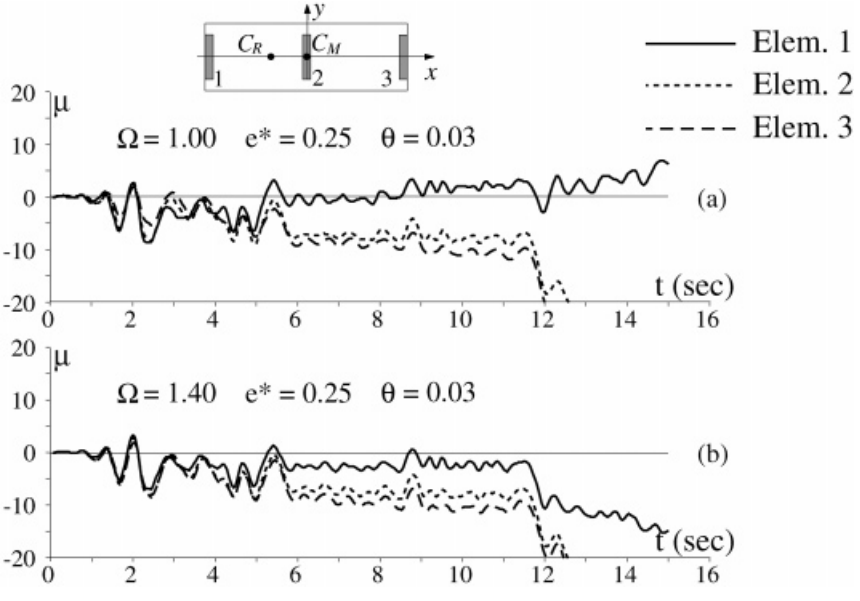

Figure 8. Element ductility demand time histories for systems with $T = 0{\cdot}5$ sec and $R = 9$; E1 Centro record

Another way of showing the effect of Ω on R_1 and the peak ductility demand (PDD) is presented in Figure 9(a) for a CM model with a constant value of e^* ($= 0{\cdot}25$) and of T ($= 0{\cdot}5$ sec) and excited by the El Centro record. As expected, R_1 increases with Ω. Obviously, the corresponding SDOF model is characterized by the largest R_1 since in this respect it tends to behave as having $\Omega \to \infty$. A similar behaviour has been observed for SME models (not shown).

The effect of the normalized eccentricity e^* on R_1 and PDD for models having a constant value of Ω ($= 1{\cdot}0$) and subjected to the same record is shown in Figure 9(b). It can clearly be seen that R_1 is falling with increasing values of e^*.

The stability bounds R_1 for the Taft record are shown in Figure 10 for models with overstrength (10a) and without it (10b). Each of these figures displays R_1 against the lateral period T, i.e R_1 spectra, for the nine CM models described in Table I. These figures also compare the computed R_1 spectrum for the reference SDOF systems (having a natural period equal to the uncoupled period of their asymmetric counterpart) with that obtained from a variant of a statistical formula derived by Bernal.[4] For elastic–perfectly plastic SDOF systems, Bernal's formula for the acceleration $a_1(T)$ at incipient collapse is given by:

$$a_1(T) = \frac{5\bar{\theta}^{0{\cdot}75}}{T^{1{\cdot}42}}\,\mathrm{PGV}\sqrt{t_{0{\cdot}9}} \tag{11a}$$

where $\bar{\theta} = \theta_{\mathrm{eff}}$, since $r_0 = 0{\cdot}0$, and $t_{0{\cdot}9}$ = effective earthquake duration (central 90 per cent of the total energy), but need not to be larger than:

$$a_1(T) = \frac{36\bar{\theta}^{0{\cdot}75}}{T^{1{\cdot}86}}\,\mathrm{PGD}t_{0{\cdot}9}^{0{\cdot}2} \tag{11b}$$

where PGD is the Peak Ground Displacement.

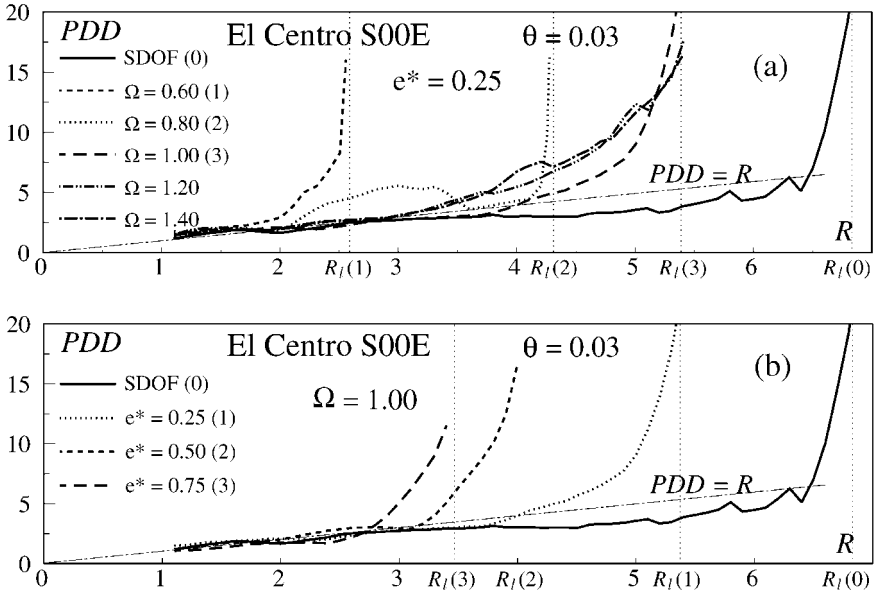

Figure 9. Effect of Ω (a); and of e^* (b) on PDD vs. R

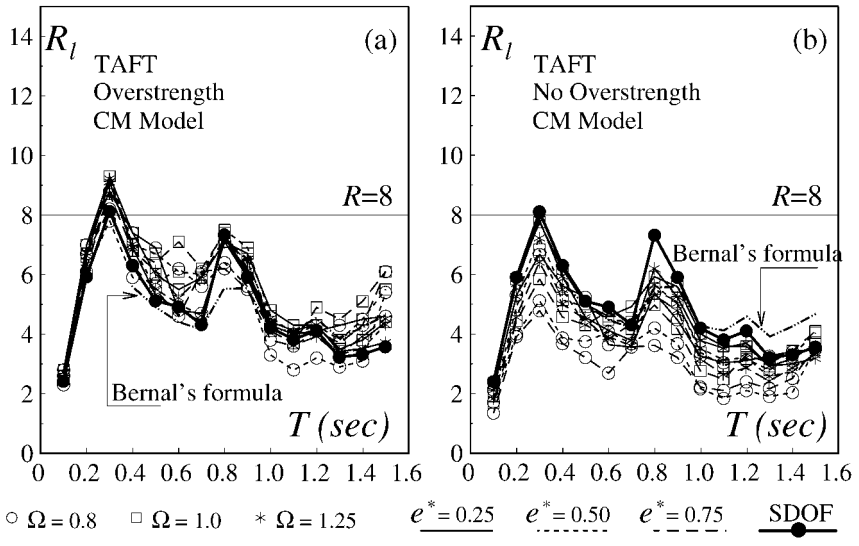

Figure 10. Stability bounds R_l for systems under Taft record: unidirectional excitation

Once $a_l(T)$ is known, the limiting reduction factor R_l can be obtained from:

$$R_l = \frac{S_a(T)}{a_l(T)} \tag{12}$$

where $S_a(T)$ is the elastic spectral acceleration for the record.

The main feature of the results with *OS* appears to be their narrow spread throughout the range of periods. This is a reflection of the adequacy of the UBC design eccentricity formulas to control the response through overstrength and judicious distribution of strength among the resisting elements.

The computed R_l values for the reference SDOF systems appear in good agreement with those predicted by Bernal's formula for its intended range ($T \geqslant 0{\cdot}4$ sec). Similar trends are observed for the other earthquakes considered.

Some insight into the expected level of R_l can be gained from Figure 10(a). Noting that $R_w = 12$ is commensurate with $R = 8$ (at limit state level), and that for the purpose of design R_l should be larger than R, it is evident that the level of R_l computed for Taft is very low. Note also the slight downward trend of the response for periods larger than 0·4 sec. To a lesser extent this behaviour is also present in the response to El Centro.[26]

The effects of *OS* on the different models can even better be appreciated from Figures 11(a) and (b), in which the mean ratio R_l (asymmetric)/R_l (symmetric) — or R_l ratio — of the five records listed in Table II is plotted against T for models with and without overstrength, respectively. The beneficial effects of *OS* are manifested in Figure 11(a). Indeed, it might be argued that the UBC overstrength is excessive, in particular at the larger T range of the R_l spectrum. Figure 11(b) shows quite clearly that for systems without *OS* having large eccentricities ($e^* \geqslant 0{\cdot}5$) combined with low Ω ($= 0{\cdot}8$), the reduction in R_l relative to the symmetric case is most

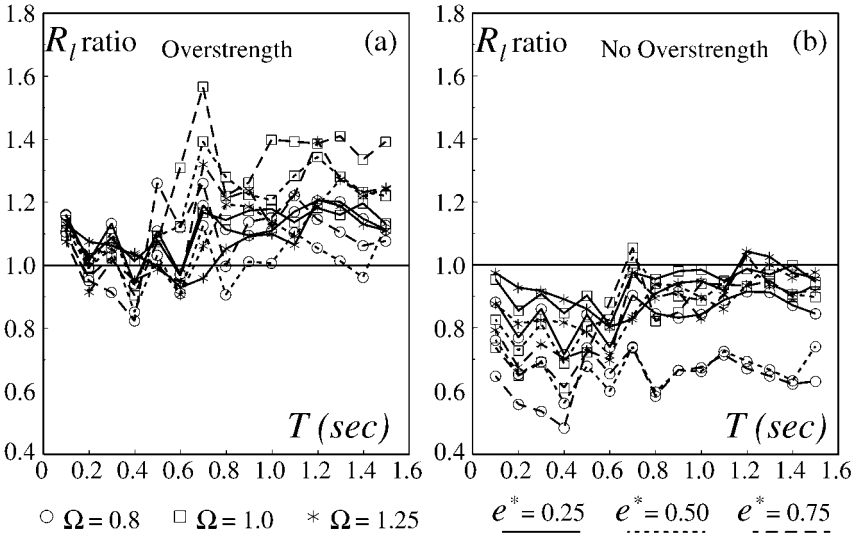

Figure 11. Mean ratio R_1 (asym.)/R_1 (sym.): Unidirectional excitation

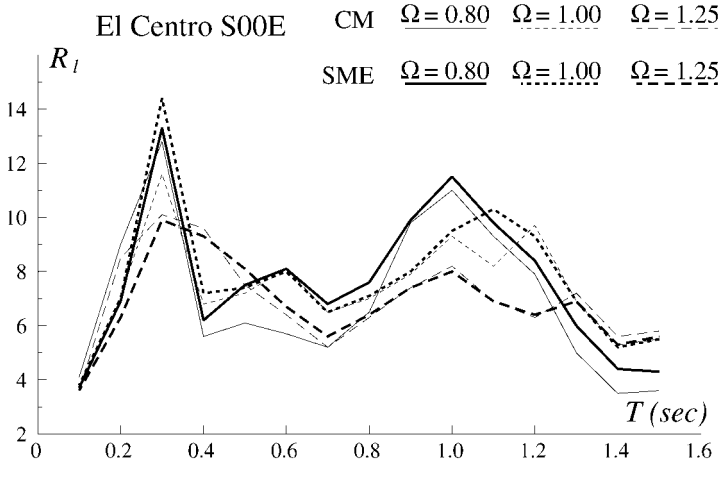

Figure 12. Comparison of limiting reduction factors R_1 between CM and SME systems; $e^* = 0{\cdot}50$

pronounced (usually more than 30 per cent). Note also the mild increase in the mean ratios as the period T elongates.

The influence of model characteristics on R_1 is shown in Figure 12 for the El Centro record. It can be seen that for an intermediate eccentricity ($e^* = 0{\cdot}50$) and a spread of Ω ($= 0{\cdot}80, 1{\cdot}00, 1{\cdot}25$)

there is a very small difference between the R_1 values of CM and SME models within the whole range of natural periods studied here.

RESULTS FOR BIDIRECTIONAL EXCITATION

Only a very limited study has been carried out for bidirectional excitation. From the ductility time histories of the resisting elements it appears that the failure mode develops in the direction along which the seismic component, leading to earlier dynamic instability of the reference SDOF system, is applied. As an example, consider the ductility demand histories of a six-element CM model (Figure 13) having the same system parameters as the model in Figure 8(a) and $T_x = T_y$, which is subjected to both components of the El Centro record. In this case $R_1 = 5{\cdot}3$, whereas for the reference SDOF system $R_1(\text{S00E}) = 7{\cdot}7$ and $R_1(\text{S90W}) = 6{\cdot}1$. Figure 13 shows that dynamic instability develops in the symmetric x-direction along which the El Centro S90W component is acting. Conversely, if the S90W component acts along the asymmetric y-direction, the failure mode develops just in that direction (not shown).

R_1 spectra have been computed for CM models under both S00E and S90W components of the El Centro record. This analysis has been limited to six-element UBC-designed CM models having $\Omega = 1{\cdot}0$ and $e^* = 0{\cdot}50$, resulting in $OS_x = 1{\cdot}09$ in the symmetric x-direction and $OS_y = 1{\cdot}31$ in the asymmetric y-direction. Two analyses have been performed: (1) 'basic', i.e. the S00E component has been assumed to act along y (as for the unidirectional case) and S90W along

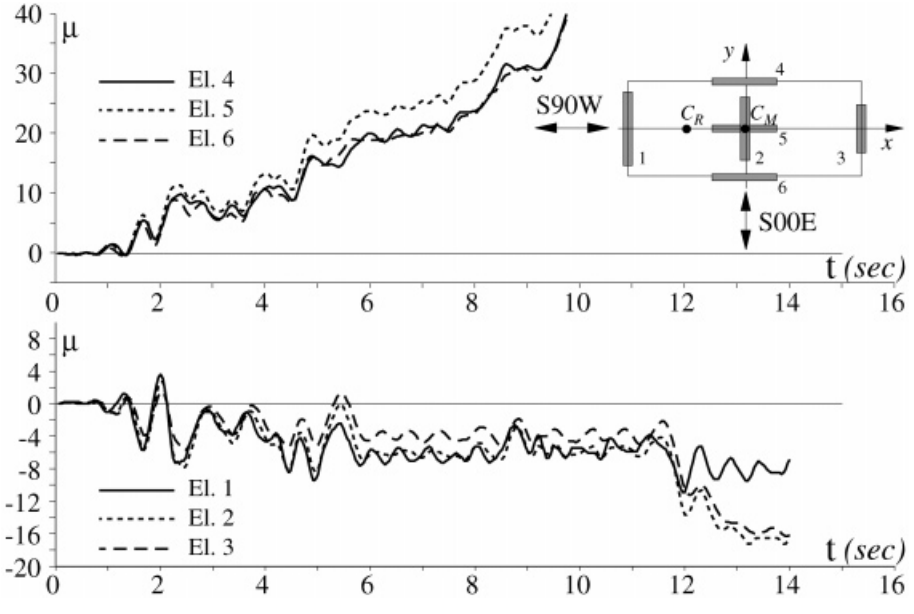

Figure 13. Element ductility demand time histories: bidirectional E1 Centro excitation

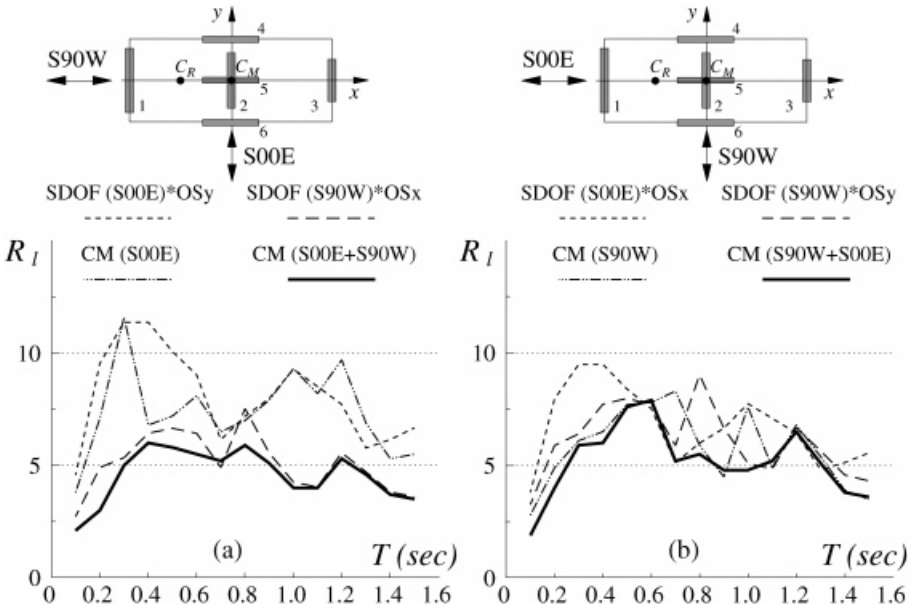

Figure 14. R_I spectra for bidirectional El Centro excitation: (a) 'basic'; (b) 'reversed' analysis

x; (2) 'reversed', i.e. the S90W component acting along y and S90W along x. Values of R_I, computed for biaxial excitation, have been compared to those obtained for reference SDOF systems under each of the two earthquake components. For the sake of consistency, since R_I values for the asymmetric CM models include the code-overstrength along both x- and y-directions, the SDOF R_I values under each of the two El Centro components have been amplified by the relevant code overstrength. Therefore, for the 'basic' analysis, SDOF R_I values for the S00E component were factored by 1·31, whereas those for S90W by 1·09, and vice versa for the 'reversed' analysis.

Results for both analyses are shown in Figure 14 for CM systems having design base shears along x- and y-directions given by the elastic spectral accelerations of the relevant earthquake component. It appears that R_I values for the asymmetric CM model under biaxial El Centro excitation, denoted as CM(S00E + S90W), are substantially affected by the lower of the two sets of SDOF R_I values, which in most cases are those for the S90W component. Therefore, for the systems under investigation, it is important to consider the simultaneous action of the two horizontal earthquake components so directed as to lead to the more adverse effect, since the S90W component appears to induce dynamic instability earlier than the S00E component, although it has a lower PGA ($= 0{\cdot}214g$).

Since $T_x = T_y$, equal base shear capacity should be allotted to the x- and y-directions (ignoring for simplicity additional overstrength due to orthogonal effects). This was done for another set of the CM(S00E + S90W) models. For consistency, the PGA level of the S90W component was scaled to that of the S00E one. The results (not shown) predict similar stability bounds as those in Figure 14.

CONCLUSIONS

This paper has been mainly concerned with the effects of gravity loads, or $P-\Delta$ effects, on the force reduction factor at the threshold of instability of elastic–plastic one-storey asymmetric structures. The following conclusions can be drawn:

1. For structures with small positive secondary response curve the stability bound R_1 can be lower than the higher values of the reduction factor R permitted by seismic codes. Therefore, R should be chosen based also on stability considerations, and not solely on the structural type. Equation (12) can be used to approximate R_1, although for design purposes a simplified version should be sought. The significance, if any, of the small fall in R_1 with the period, predicted for the Taft and El Centro records within the range studied, should be further explored.
2. In asymmetric structures gravity effects are amplified due to torsion. Yet, based on studies of one-storey asymmetric models designed by the seismic provisions of UBC 1994, this study shows that the torsional effects are neutralized by overstrength and the judicious distribution of total strength among the resisting elements. As a result, R_1 values are similar to or even higher than those for their symmetric counterparts. It follows that for asymmetric systems of the type studied herein R_1 can also be approximately predicted by equation (12).
3. Model characteristics, i.e. stiffness vs. mass eccentricity, do not affect R_1 appreciably.
4. When considering bidirectional excitation, R_1 values are closer to the lower of the two values computed separately, i.e. unidirectionally for each component. Therefore, equation (12) appears to be applicable also for systems under two-component earthquakes.
5. Finally, R_1 and therefore the stability bound on R, depends on the hysteretic and degrading force–displacement characteristics of the structure. This paper presents results only for bilinear elastic–plastic models. Therefore, a recommendation for modifying the code prescribed R values requires that similar studies be carried out on degrading systems.

ACKNOWLEDGEMENTS

The authors thank the two anonymous reviewers for their constructive criticism. They also acknowledge the support of the Italian CNR and the Israeli Ministry of Construction and Housing for the work reported herein.

REFERENCES

1. *NEHRP*, *Recommended Provisions for the Development of Seismic Regulations for New Buildings 1994 Edition*, Federal Emergency Management Agency, Part 1 — Provisions FEMA 222A, and Part 2 — Commentary FEMA 223A (1995).
2. D. Bernal, 'Amplification factors for inelastic dynamic P–Δ effects in earthquake analysis', *Earthquake Engng. Struct. Dyn.* **15**, 635–651 (1987).
3. E. Cosenza, A. De Luca, C. Faella and V. Piluso, 'A rational formulation for the q-factor in steel structures', *Proc. 11th WCEE*, Tokyo-Kyoto, Japan, 1988.
4. D. Bernal, 'Instability of buildings subjected to earthquakes', *J. Struct. Engng. ASCE* **118**, 2239–2260 (1992).
5. M. Rahnama and H. Krawinkler, 'Effect of Soft Soil and Hysteresis Model on Seismic Demand', *Report 108*, John A. Blume Earthquake Engineering. Center, Stanford University, 1993.
6. G. A. MacRae, 'P–Δ effects on single-degree-of-freedom structures in earthquakes', *Earthquake Spectra* **10** (3), 539–568 (1994).
7. S. Mahin and R. Boroschek, 'Influence of geometric nonlinearities on the seismic response and design of bridge structures', *Background Report to California Dept. of Transportation*, Div. of Structures, 1991.
8. M. J. N. Priestley, F. Seible and G. M. Calvi, *Seismic Design and Retrofit of Bridges*, Wiley, New York, U.S.A., 1996.

9. R. C. Fenwick, B. J. Davidson and B. T. Chung, 'P-Delta action in seismic resistant structures', *Bull. New Zealand Nat. Soc. Earthquake Engng.* **25** (1992).
10. F. M. Mazzolani and V. Piluso, '*P*–Δ effect in seismic resistant steel structures', *Proc. SSRC Annual Technical Session and Meeting*, Milwaukee, U.S.A., 1993.
11. E. Sordo and D. Bernal, 'Effect of torsional coupling on stability of structures', *Proc. 10th WCEE*, Vol. 7, Balkema, 1992, pp. 3859–3864.
12. E. Sordo and D. Bernal, 'Dynamic instability in three dimensional structures', *Report No. CE-94-14*, Department of Civil Engineering, Northeastern University, Boston, MA, 1994.
13. *Uniform Building Code*, Int. Conf. of Building Officials, ICBO, Whittier, CA, 1994.
14. A. Rutenberg, A. Benbenishti and O. Pekau, 'Nonlinear seismic behavior of code-designed eccentric systems', *Proc. 10th WCEE*, Vol. 10, Balkema, 1992, pp. 5751–5756.
15. M. De Stefano, G. Faella and R. Ramasco, 'Inelastic response and design criteria of plan-wise asymmetric systems', *Earthquake Engng. Struct. Dyn.* **22**, 245–259 (1993).
16. J. C. Correnza, G. L. Hutchinson and A. M. Chandler, 'Effect of transverse load-resisting elements on inelastic earthquake response of eccentric-plan buildings', *Earthquake Engng. Struct. Dyn.* **23**, 75–89 (1994).
17. J. C. De la Llera and A. K. Chopra, 'Understanding the inelastic seismic behavior of asymmetric-plan buildings', *Earthquake Engng. Struct. Dyn.* **24**, 549–572 (1995).
18. A. Rutenberg, 'Simplified *P*–Δ analyses for asymmetric structures', *J. Struct. Div. ASCE* **107**, 1995–2013 (1982).
19. Seismology Committee, Structural Engineers Association of California, *Recommended Lateral Force Requirements and Commentary*, Sacramento, CA, 1996.
20. C. M. Wong and W. K. Tso, 'Evaluation of seismic torsional provisions in Uniform Building Code', *J. Struct. Engng. ASCE* **121**, 1436–1442 (1995).
21. M. De Stefano and A. Rutenberg, 'A comparison of the present SEAOC/UBC torsional provisions with the old ones', *Engng. Struct.* **19**, 655–664 (1997).
22. A. Rutenberg, 'Nonlinear response of asymmetric building structures and seismic codes: a state of the art review', *Eur. Earthquake Engng.* **2**, 3–19 (1992).
23. A. Rutenberg and M. De Stefano, 'On the seismic stability of asymmetric code-designed structures', *Proc. Pacific Conf. on Earthquake Engineering*, Melbourne, 1995.
24. A. E. Kanaan and G. H. Powell, 'DRAIN2D-General purpose computer program for dynamic analysis of inelastic plane structures', *Report No. EERC 73-6* and *73-22*, Earthquake Engrg. Res. Center, University of California, Berkeley, U.S.A., 1973.
25. D. P. Mondkar and G. H. Powell, 'ANSR-I - General purpose computer program for analysis of nonlinear structural response', *Report No. EERC 75-37*, Earthquake Engineering Research Center, University of California, Berkeley, U.S.A., 1975.
26. M. De Stefano and A. Rutenberg, 'Seismic instability and the force reduction factor of yielding structures', *Proc. 11th WCEE*, Paper No. 1137, Acapulco, Mexico, Elsevier, 1996.

